ORIGINAL ARTICLE

Loss of DP1 Aggravates Vascular Remodeling in Pulmonary Arterial Hypertension via mTORC1 Signaling

Yuhu He[1,2,3*], Caojian Zuo[3,4*], Daile Jia[3,5*], Peiyuan Bai[3,5*], Deping Kong[1*], Di Chen[3*], Guizhu Liu[6], Juanjuan Li[3], Yuanyang Wang[1], Guilin Chen[1], Shuai Yan[3], Bing Xiao[3], Jian Zhang[1], Lingjuan Piao[3], Yanli Li[1], Yi Deng[1], Bin Li[7], Philippe P. Roux[8,9], Katrin I. Andreasson[10], Richard M. Breyer[11,12], Yunchao Su[13], Jian Wang[6‡], Ankang Lyu[5‡], Yujun Shen[1‡], and Ying Yu[1,3,6‡]

[1]Department of Pharmacology, Tianjin Key Laboratory of Inflammation Biology, Key Laboratory of Immune Microenvironment and Disease (Ministry of Education), School of Basic Medical Sciences, Tianjin Medical University, Tianjin, China; [2]Department of Cardiovascular Medicine, Second Xiangya Hospital, Central South University, Changsha, Hunan, China; [3]Chinese Academy of Sciences Key Laboratory of Nutrition, Metabolism and Food Safety, Shanghai Institute of Nutrition and Health, Shanghai Institutes for Biological Sciences, University of Chinese Academy of Sciences, Chinese Academy of Sciences, Shanghai, China; [4]Department of Cardiology, Shanghai General Hospital, and [5]Department of Cardiology, Ruijin Hospital, Shanghai Jiaotong University School of Medicine, Shanghai, China; [6]State Key Laboratory of Respiratory Diseases, Guangzhou Institute of Respiratory Health, First Affiliated Hospital of Guangzhou Medical University, Guangzhou, Guangdong, China; [7]Orthopedic Institute, Soochow University, Jiangsu, China; [8]Institute for Research in Immunology and Cancer and [9]Department of Pathology and Cell Biology, University of Montreal, Montreal, Quebec, Canada; [10]Department of Neurology and Neurological Sciences, Stanford University School of Medicine, Stanford, California; [11]Department of Veterans Affairs, Tennessee Valley Health Authority, Nashville, Tennessee; [12]Department of Medicine, Vanderbilt University Medical Center, Nashville, Tennessee; and [13]Department of Pharmacology and Toxicology, Medical College of Georgia, Augusta University, Augusta, Georgia

ORCID IDs: 0000-0002-1278-256X (J.W.); 0000-0001-6662-8624 (A.L.); 0000-0002-9266-9064 (Y.S.); 0000-0002-6476-1752 (Y.Y.).

Abstract

Rationale: Vascular remodeling, including smooth muscle cell hypertrophy and proliferation, is the key pathological feature of pulmonary arterial hypertension (PAH). Prostaglandin I_2 analogs (beraprost, iloprost, and treprostinil) are effective in the treatment of PAH. Of note, the clinically favorable effects of treprostinil in severe PAH may be attributable to concomitant activation of DP1 (D prostanoid receptor subtype 1).

Objectives: To study the role of DP1 in the progression of PAH and its underlying mechanism.

Methods: DP1 levels were examined in pulmonary arteries of patients and animals with PAH. Multiple genetic and pharmacologic approaches were used to investigate DP1-mediated signaling in PAH.

Measurements and Main Results: DP1 expression was downregulated in hypoxia-treated pulmonary artery smooth muscle cells and in pulmonary arteries from rodent PAH models and patients with idiopathic PAH. *DP1* deletion exacerbated pulmonary artery remodeling in hypoxia-induced PAH, whereas pharmacological activation or forced expression of the DP1 receptor had the opposite effect in different rodent models. *DP1* deficiency promoted pulmonary artery smooth muscle cell hypertrophy and proliferation in response to hypoxia via induction of mTORC1 (mammalian target of rapamycin complex 1) activity. Rapamycin, an inhibitor of mTORC1, alleviated the hypoxia-induced exacerbation of PAH in DP1-knockout mice. DP1 activation facilitated raptor dissociation from mTORC1 and suppressed mTORC1 activity through PKA (protein kinase A)-dependent phosphorylation of raptor at Ser791. Moreover, treprostinil treatment blocked the progression of hypoxia-induced PAH in mice in part by targeting the DP1 receptor.

Conclusions: DP1 activation attenuates hypoxia-induced pulmonary artery remodeling and PAH through PKA-mediated dissociation of raptor from mTORC1. These results suggest that the DP1 receptor may serve as a therapeutic target for the management of PAH.

Keywords: pulmonary arterial hypertension; DP1 receptor; pulmonary artery smooth muscle cell; hypertrophy and proliferation; mTOR signaling

(Received in original form November 6, 2019; accepted in final form January 8, 2020)

*These authors contributed equally to this work.

‡These authors contributed equally to this work as senior authors.

Correspondence and requests for reprints should be addressed to Ying Yu, M.D., Ph.D., or Yujun Shen, Ph.D., Department of Pharmacology, School of Basic Medical Sciences, Tianjin Medical University, 22 Qixiangtai Road, Heping District, Tianjin 300070, China. E-mail: yuying@tmu.edu.cn (Y.Y.) or yujun_shen@tmu.edu.cn (Y.S.).

This article has a related editorial.

This article has an online supplement, which is accessible from this issue's table of contents at www.atsjournals.org.

Am J Respir Crit Care Med Vol 201, Iss 10, pp 1263–1276, May 15, 2020

Originally Published in Press as DOI: 10.1164/rccm.201911-2137OC on January 9, 2020
Internet address: www.atsjournals.org

At a Glance Commentary

Scientific Knowledge on the Subject: Pulmonary arterial hypertension (PAH) is a devastating disease characterized by pulmonary vascular remodeling such as smooth muscle cell hypertrophy and proliferation. Prostaglandin I_2 analogs (beraprost, iloprost, and treprostinil) are effective in the treatment of PAH. Prostaglandin D_2 exerts proresolution and vasodilatory effects via DP1 (D prostanoid receptor subtype 1). Treprostinil is also a potent DP1 agonist. It remains unknown whether the clinically favorable effects of treprostinil in severe PAH are attributable to concomitant activation of the DP1 receptor.

What This Study Adds to the Field: In this study, we demonstrate that DP1 expression was downregulated in pulmonary arteries in various animal models of PAH and in patients with idiopathic PAH. Ablation of the DP1 receptor exacerbated hypoxia-induced PAH and enhanced pulmonary artery remodeling in mice through activation of mTORC1 (mammalian target of rapamycin complex 1) signaling. DP1 activation facilitated mTORC1 dissociation and suppressed mTORC1 activity in pulmonary artery smooth muscle cells through PKA (protein kinase A)-dependent phosphorylation of raptor at Ser791. We also found that treprostinil exerted therapeutic effects on PAH in mice in part through the DP1 receptor. These findings suggest that the DP1 receptor is a potential therapeutic target for PAH treatment.

Pulmonary arterial hypertension (PAH) is a progressive and lethal pulmonary vascular disease characterized by severe distal pulmonary artery (PA) remodeling and increased pulmonary vascular resistance that eventually lead to right-sided heart failure. Endothelial dysfunction, smooth muscle cell hyperplasia and hypertrophy, extracellular matrix deposition, and perivascular inflammatory infiltrate contribute to PA remodeling in PAH (1). Current available therapies such as endothelin receptor antagonists, phosphodiesterase inhibitors, and prostacyclin analogs predominantly target pulmonary vasoconstriction and improve PAH symptoms, but the mortality rate remains unsatisfactory. Identifying novel pathways involved in pulmonary vascular remodeling can reveal novel therapeutic targets, which can lead to improved clinical outcomes (2).

Arachidonic acid metabolites play a critical role in maintaining pulmonary vascular homeostasis. Cyclooxygenase (COX) catalyzes the transformation of arachidonic acid into prostaglandins (PGs), including PGE_2, PGD_2, $PGF_{2\alpha}$, and PGI_2 (prostacyclin), and thromboxane, all of which exert their physiological and pathophysiological functions through activation of the cognate G protein–coupled receptor (i.e., PGE_2 receptors [EP1–EP4], PGD_2 receptors [D prostanoid receptor subtypes 1 and 2; DP1 and DP2], $PGF_{2\alpha}$ receptor, PGI_2 receptor [IP], and thromboxane receptor). Loss of COX-2 exacerbates hypoxia-induced PAH in mice by increasing vascular smooth muscle cell (VSMC) contractility (3). In the clinic, PGI_2 analogs and IP receptor agonists are widely used to manage PAH. Currently employed IP agonists include synthetic PGI_2 (epoprostenol), stable PGI_2 analogs (beraprost, iloprost, and treprostinil), and a highly selective IP agonist (selexipag) (4). Like endogenous PGI_2, synthetic epoprostenol is unstable at room temperature and has a very short half-life. In contrast, selexipag, which is chemically distinct from PGI_2, is an orally delivered, potent, nonprostanoid IP receptor agonist (5). As an inhaled medication, treprostinil exerts a more sustained effect on pulmonary vascular resistance with higher tolerability at relatively low doses than iloprost (6), and clinical observations have shown that transitioning from inhaled iloprost to treprostinil markedly improves quality of life in patients with PAH (7).

The three analogs have heterogeneous binding affinities for other PG receptors, which may confer variable clinical efficacy (8, 9). For example, nonspecific binding and activation of the EP3 receptor could decrease the long-term tolerability and efficacy of PGI_2 analogs (10, 11). Despite a longer half-life, treprostinil has much higher affinity than iloprost for the vasodilator DP1 and EP2 receptors (9). On the one hand, DP1 is expressed in both human PAs and veins, and its activation induces relaxation of human pulmonary vessels (12); on the other hand, EP2 suppresses endothelin 1–stimulated proliferation of human pulmonary artery smooth muscle cells (hPASMCs) *in vitro* (13). Thus, DP1 antagonists inhibit the relaxation of human PAs induced by treprostinil, suggesting that they could mediate the therapeutic effects of treprostinil in patients with PAH (14). However, whether DP1 and EP2 receptors are involved in the pathogenesis of PAH remains to be determined.

In this study, we demonstrate that DP1 expression is downregulated in PAs in various animal models of PAH and in patients with idiopathic PAH. Ablation of the DP1 receptor exacerbated hypoxia-induced PAH in mice by enhancing mTORC1 (mammalian target of rapamycin complex 1) activity. We also found that treprostinil exerts therapeutic effects on PAH in mice in part through DP1. These findings suggest that DP1 is a potential therapeutic target for PAH treatment.

Methods

Extended description of the methods is provided in the online supplement.

Animals

Eight- to 10-week-old male mice and rats were used in all experiments in this study. Wild-type (WT), IP-knockout ($IP^{-/-}$), *DP1*-knockout ($DP1^{-/-}$), and *EP2*-knockout

Supported by the National Key R&D Program of China (no. 2017YFC1307404), the National Natural Science Foundation of China (nos. 81790623, 81525004, 91439204, 81930002, 81630004, and 81800059), the Natural Science Foundation of Tianjin (no. 17JCYBJC40700), and the NIH (HL134895, HL115078, and HL134934). Y.Y. is a fellow at the Jiangsu Collaborative Innovation Center for Cardiovascular Disease Translational Medicine.

Author Contributions: Y.H., J.W., A.L., Y. Shen, and Y.Y. designed research. Y.H., Y. Shen, and Y.Y. wrote the paper. Y.H., C.Z., D.J., P.B., D.K., D.C., G.L., J.L., Y.W., G.C., S.Y., B.X., Y.D., and B.L. conducted experiments. D.K., J.Z., L.P., Y.L., J.W., A.L., Y. Shen, and Y.Y. analyzed the data. P.P.R., K.I.A., R.M.B., and Y. Su provided important reagents and tissue samples.

($EP2^{-/-}$) mice were maintained on a C57BL/6 genetic background. $DP1^{-/-}$ and $IP^{-/-}$ mice were mated to generate the double-knockout ($DP1^{-/-}IP^{-/-}$) mice. VSMC-specific $DP1^{-/-}$ mice ($DP1^{F/F}SM22^{Cre}$) were generated by crossing $DP1^{F/F}$ mice (15) with SM22-Cre–transgenic mice (10). WT littermates of each strain were generated as experimental control animals by mating heterozygotes. Mice were maintained in an environment with controlled temperature ($22 \pm 1^{\circ}C$) and relative humidity ($50 \pm 5\%$) on a 12-h light and 12-h dark cycle and with free access to sterile food and water. Animal experiments were approved by the institutional animal care and use committee of the Institute for Nutritional Sciences, University of Chinese Academy of Sciences.

Rodent Models of PAH

A hypoxia- or hypoxia + SU5416 (HySu)-induced mouse model of PAH and a monocrotaline (MCT)-induced rat model of PAH were used to examine PAH development. In all animal experiments, littermates or vehicle-treated animals were used as controls. For the hypoxia-induced PAH model, 8–10-week-old male mice maintained on normal chow were exposed to 10% O_2 (hypoxia) or room air (normoxia) for 3 weeks as previously described (10). To restore DP1 expression, 1 week before hypoxia induction, lentivirus encoding DP1 (3×10^8 transduction units in 30 μl of phosphate-buffered saline) was injected into the trachea of $DP1^{-/-}$ mice, followed by injection of air, to promote the spread of virus throughout the lungs (16). For rapamycin treatment, mice were administered an intraperitoneal injection with rapamycin at 3 mg/kg every other day during the 3-week hypoxia exposure period (17).

For the HySu model, mice were administered a subcutaneous injection with the vascular endothelial growth factor receptor inhibitor SU5416 (20 mg/kg body weight) under isoflurane anesthesia, followed by exposure to hypoxia (10% O_2) for 3 weeks, according to methodology in a previous report (18). An Alzet osmotic minipump (DURECT Corporation) filled with either treprostinil (infusion rate, 30 $ng \cdot kg^{-1} \cdot min^{-1}$) or sterile 0.9% injectable saline and equilibrated at 37°C in phosphate-buffered saline for 48 hours was subcutaneously implanted into the mice (19), which were subjected to HySu treatment 3 days later.

At the end of the treatment, animals were anesthetized; a 1.2-French (for mice) or 1.4-French (for rats) microtip pressure transducer catheter (Millar Instruments) was carefully inserted into the right ventricle (RV); and right ventricular systolic pressure (RVSP) was continuously monitored for 5 minutes using a PowerLab data acquisition system (ADInstruments). Right ventricular hypertrophy was assessed by Fulton index measurements (weight of RV/weight of left ventricle plus septum [RV/LV + S]).

Statistical Analysis

Data are expressed as mean ± SEM and were analyzed using Prism version 5.0 software (GraphPad Software Inc.). A two-tailed unpaired Student's *t* test and one- or two-way ANOVA with a Bonferroni *post hoc* test were used to compare the means of different groups. $P < 0.05$ was considered statistically significant. Randomization and blind analyses were used whenever possible.

Results

DP1 Receptor Is Downregulated in PAs from PAH Rodent Models and Patients with Idiopathic PAH

COX-2 expression is upregulated in lung tissues from patients with PAH and in PAs from mice with hypoxia-induced PAH (10, 20). Accordingly, we found that all PG products were upregulated in the lungs of mice in response to chronic hypoxia (Figures E1A–E1E in the online supplement). On the one hand, *DP1* deficiency had no impact on PG generation. On the other hand, DP1, but not DP2, mRNA expression was markedly reduced in PAs from chronic hypoxia–treated mice and MCT-treated rats (Figures 1A and 1B) and in murine pulmonary artery smooth muscle cells (mPASMCs) cultured under hypoxic conditions (Figure 1C), whereas DP2 expression was unchanged. Similarly, DP1 expression was downregulated in hPASMCs in response to hypoxia (Figure 1D). DP1 protein, mainly located in the smooth muscle cell layer (Figure 1E), was downregulated in PAs from hypoxia-treated mice (Figures 1E and 1F). Consistently, we also observed that DP1 expression was reduced in PAs from patients with idiopathic PAH as compared with those from healthy individuals (Figures 1G and 1H).

Then we explored the underlying mechanisms for hypoxia-induced DP1 downregulation using the mouse vascular smooth muscle (MOVAS) cell line (Figure E2A). Multiple potential transcription factor–binding motifs for HIF-1α (hypoxia-inducible factor 1α), BCL6 (B-cell lymphoma 6), Egr1 (early growth response protein 1), and Creb1 (cAMP-responsive element–binding protein 1) were predicted in the DP1 gene promoter region using FindM software (https://ccg.epfl.ch/ssa/findm.php) (Figure E2B). Indeed, hypoxia increased the expression of the four transcription factors (Figures E2C–E2F). However, knockdown of either HIF-1α or BCL6, but not Creb1 and Egr1, markedly attenuated hypoxia-triggered DP1 downregulation in MOVAS cells (Figures E2G–E2N). Through chromatin immunoprecipitation assay, we observed that hypoxia treatment dramatically increased HIF-1α and BCL6 binding activity on the DP1 promoter region at −3,651 to −3,636 bp (Figures E3A–E3C) and at −3,826 to −3,807 bp, respectively (Figures E3A and E3C). Interestingly, HIF-1α interacted with BCL6 in MOVAS cells (Figures E3D and E3E). Thus, hypoxia suppressed DP1 expression in VSMCs, probably through HIF-1α–mediated recruitment of inhibitory transcription factor BCL6 (Figure E3F).

Deletion of DP1 but Not EP2 Exacerbates Hypoxia-induced PAH in Mice

To explore the role of the vasodilator DP1 and EP2 receptors in the development of PAH, we performed pulmonary hemodynamic and histological analyses in chronic hypoxia–challenged $DP1^{-/-}$ and $EP2^{-/-}$ mice. The $DP1^{-/-}$ mice developed more severe PAH, with significant increases in RVSP (Figure E4A) and in the RV/LV + S ratio (Figure E4B) relative to WT control mice. Moreover, *DP1* deficiency enhanced hypoxia-induced pulmonary vascular remodeling in both small PAs and arterioles, as evidenced by increased pulmonary vascular wall thickness and muscularization (Figures E4C–E4H). Notably, $DP1^{-/-}$ mice had enlarged PASMCs after chronic hypoxia challenge (Figure E4I), with increased ACTA2 (α-smooth muscle actin) expression (Figures E4J and E4K) and deposition of perivascular matrix proteins

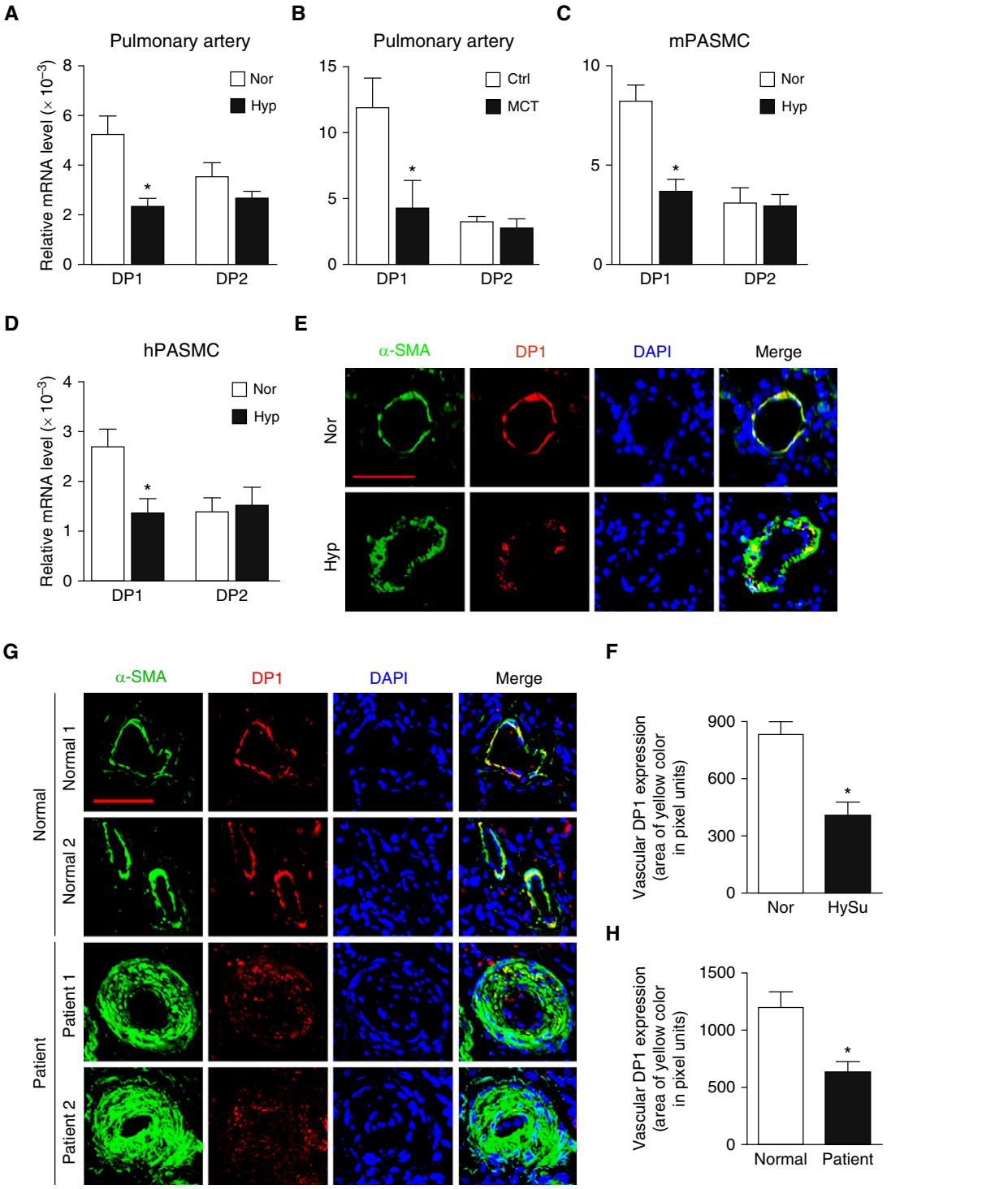

Figure 1. DP1 (D prostanoid receptor subtype 1) is downregulated in pulmonary artery smooth muscle cells in response to hypoxia. (*A*) Relative mRNA concentrations of DP1 and DP2 in lung pulmonary arteries from mice subjected to chronic hypoxia (Hyp). *$P < 0.05$ versus normoxia (Nor) ($n = 7$–10). (*B*) Relative mRNA concentrations of DP1 and DP2 in lung pulmonary arteries from monocrotaline (MCT)-treated rats. *$P < 0.05$ versus control (Ctrl) ($n = 5$–7). (*C*) Relative mRNA concentrations of DP1 and DP2 in cultured murine pulmonary artery smooth muscle cells (mPASMCs) in response to hypoxia. *$P < 0.05$ versus Ctrl ($n = 5$). (*D*) Relative mRNA concentrations of DP1 and DP2 in cultured human pulmonary artery smooth muscle cells (hPASMCs) in response to hypoxia. *$P < 0.05$ versus Ctrl ($n = 5$–6). (*E*) Representative immunofluorescence images of DP1 (red) and α-SMA (α-smooth muscle actin) (green) expression in lung tissue from hypoxia-treated mice. Scale bar, 25 μm. (*F*) Quantification of DP1 expression in *E*. *$P < 0.05$ versus normal ($n = 7$). (*G*) Representative immunofluorescence images of DP1 (red) and α-SMA (green) expression in lung tissue from patients with pulmonary arterial hypertension. Scale bar, 25 μm. (*H*) Quantification of DP1 expression in *F*. *$P < 0.05$ versus normal ($n = 7$). Data represent mean ± SEM. Statistical significance was evaluated with the two-tailed Student's *t* test. HySu = hypoxia/SU5416.

such as fibronectin and type I collagen (Figures E5A–E5C). Similarly, the exaggerated PAH was induced in VSMC-specific deficient mice ($DP1^{F/F}SM22^{Cre}$) by HySu challenge (Figures 2A–2J). $DP1^{-/-}$ mPASMCs were larger and had higher protein/DNA ratios than control cells in response to hypoxia (Figures E6A–E6C). Treatment with the DP1 inhibitor BWA868C promoted hypoxia-induced hypertrophy in hPASMCs (Figures E6D–E6F). We also observed enhanced proliferation of cultured $DP1^{-/-}$ mPASMCs and DP1 inhibitor–treated hPASMCs under hypoxic conditions (Figures E6G and E6H), but we failed to detect significant increases of proliferating cell nuclear antigen–positive $ACTA2^{+}$ cells in the PAs from chronic hypoxia–treated $DP1^{-/-}$ mice compared with WT control animals (Figures E6I and E6J). In addition, there were no overt differences in pulmonary infiltration of $CD11b^{+}$ and $CD68^{+}$ inflammatory cells into perivascular areas between $DP1^{-/-}$ and WT mice after chronic hypoxia challenge (Figures E7A and E7B). However, *EP2* deficiency had no significant influence on hypoxia-induced PAH and PA remodeling in mice (Figures E8A–E8D).

Reexpression of DP1 in Lungs Attenuates PAH Exacerbation Induced by Hypoxia in $DP1^{-/-}$ Mice

Infection with DP1-expressing lentivirus via the trachea restored DP1 expression in PAs of $DP1^{-/-}$ mice (Figures E9A and E9B). As predicted, reintroduction of DP1 attenuated hypoxia-induced pulmonary hypertension in $DP1^{-/-}$ mice, as indicated by the decreased RVSP and RV/LV + S (Figures E9C and E9D) and suppression of pulmonary vascular remodeling through a reduction in wall thickness and muscularization (Figures E9E–E9G). Importantly, forced expression of DP1 also suppressed the enhancement of PASMC hypertrophy in $DP1^{-/-}$ mice with PAH (Figure E9H).

Pharmacological Activation of DP1 Inhibits Progression of MCT-induced PAH and PA Remodeling in Rats

We next examined the therapeutic effects of the DP1-specific agonist BW245C on PAH and pulmonary vascular remodeling in MCT-treated rats. BW245C (50 μg/kg twice per day) was administered to the rats twice daily starting from the beginning of the third week after MCT treatment (Figure 3A). MCT challenge markedly increased PA pressure in rats starting from Week 2 (10). Notably, BW245C administration significantly attenuated the increases in RVSP, RV/LV + S ratio, and pulmonary vascular wall thickness in MCT-treated rats (Figures 3B–3F), and it reversed PASMC hypertrophy and proliferation in PAs (Figures 3G–3I).

DP1 Deficiency Promotes Hypoxia-induced PASMC Proliferation and Hypertrophy by Increasing mTORC1 Activity in a Protein Kinase A–Dependent Manner

Chronic hypoxia activates multiple proliferative signaling in VSMCs, including MAPK (mitogen-activated protein kinase) and mTOR pathways (21). *DP1* deficiency had no effect on MAPK activation in cultured PASMCs under hypoxic and normoxic conditions, as determined by evaluating ERK1/2 (extracellular signal-regulated kinase ½), JNK (Janus kinase), and p38 protein phosphorylation degrees (Figure E10). In contrast, mTORC1, a key regulator of protein synthesis in response to growth factors and nutrients, was activated in hypoxia-treated $DP1^{-/-}$ PASMCs, as evidenced by increased phosphorylation of mTOR and its downstream target S6K (p70 ribosomal protein S6 kinase) (Figures 4A and 4B), as well as in the lungs and PAs of chronic hypoxia–challenged $DP1^{-/-}$ mice relative to their WT counterparts (Figures E11A and E11B). However, *DP1* deficiency had no effect on mTORC2 activity in PASMCs, as determined by AKT phosphorylation at Ser473 (Figure E12). Forced expression of DP1 (Figure 4C) attenuated the increase in mTORC1 activity in hypoxia-treated $DP1^{-/-}$ PASMCs (Figures 4C and 4D).

mTORC1 is composed of mTOR, raptor, and GβL (G protein β-subunit–like protein) as well as the inhibitory PRAS40 (proline-rich Akt substrate 40). A well-established upstream regulator of mTORC1 is the PI3K (phosphatidylinositol-3-kinase)/AKT signaling pathway that phosphorylates PRAS40 or tuberous sclerosis complex, another negative regulator of mTORC1 (22). Unexpectedly, we did not observe an increase in AKT activity or PRAS40 phosphorylation in $DP1^{-/-}$ mPASMCs under hypoxic and normoxic conditions as compared with WT mPASMCs (Figure E13A). Accordingly, PI3K inhibition failed to reverse the hypoxia-induced reduction in mTORC1 activity in DP1-overexpressing mPASMCs (Figure E13B). Like AKT, AMPK (5′-AMP–activated protein kinase) directly communicates with mTORC1 through phosphorylation of raptor, leading to the allosteric inhibition of the complex (23). However, we did not detect any changes in AMPK activity or raptor phosphorylation at Ser792 in $DP1^{-/-}$ mPASMCs (Figures E14A and E14B).

DP1 is connected to the cAMP signaling cascade through $G_{\alpha s}$ protein (24). *DP1* deletion reduced cAMP production in mPASMCs in response to DP1 agonist treatment (Figure 4E). cAMP/PKA (protein kinase A) signaling has been shown to suppress mTOR activity (25, 26). We also found that PKA inhibition restored mTORC1 activity in DP1-reexpressing $DP1^{-/-}$ mPASMCs in response to hypoxia (Figure 4F).

Inhibition of mTOR Alleviates PAH Exacerbation Induced by Hypoxia in $DP1^{-/-}$ Mice

Treatment with the mTOR inhibitor rapamycin abolished the increases in proliferation and hypertrophy (Figures E15A and E15B), as well as the enhancing cell traction force (Figures E15C and E15D), in cultured $DP1^{-/-}$ mPASMCs under hypoxia. In addition, rapamycin reduced the degree of pulmonary hypertension (Figures 5A and 5B), PA remodeling (Figures 5C–5F), and PASMC hypertrophy in chronic hypoxia–challenged $DP1^{-/-}$ mice (Figures 5G–5I).

DP1 Deficiency Enhances mTORC1 Activity in mPASMCs via PKA-mediated mTORC1 Dissociation

The integrity of the mTOR complex is essential for its kinase activity and signal transduction (27). To investigate whether *DP1* deficiency enhances mTORC1 activity by influencing the association of mTOR with raptor and PRAS40, mTOR was immunoprecipitated from hypoxia-treated mPASMCs, and the blot was probed with antibodies against mTOR, raptor, PRAS40, and GβL. *DP1* deficiency enhanced the binding of raptor to mTOR in mPASMCs in response to hypoxia, which was accompanied by increased mTOR activity and S6K phosphorylation (Figure 6A). Reintroducing DP1 into these cells abolished mTORC1 activation by inducing

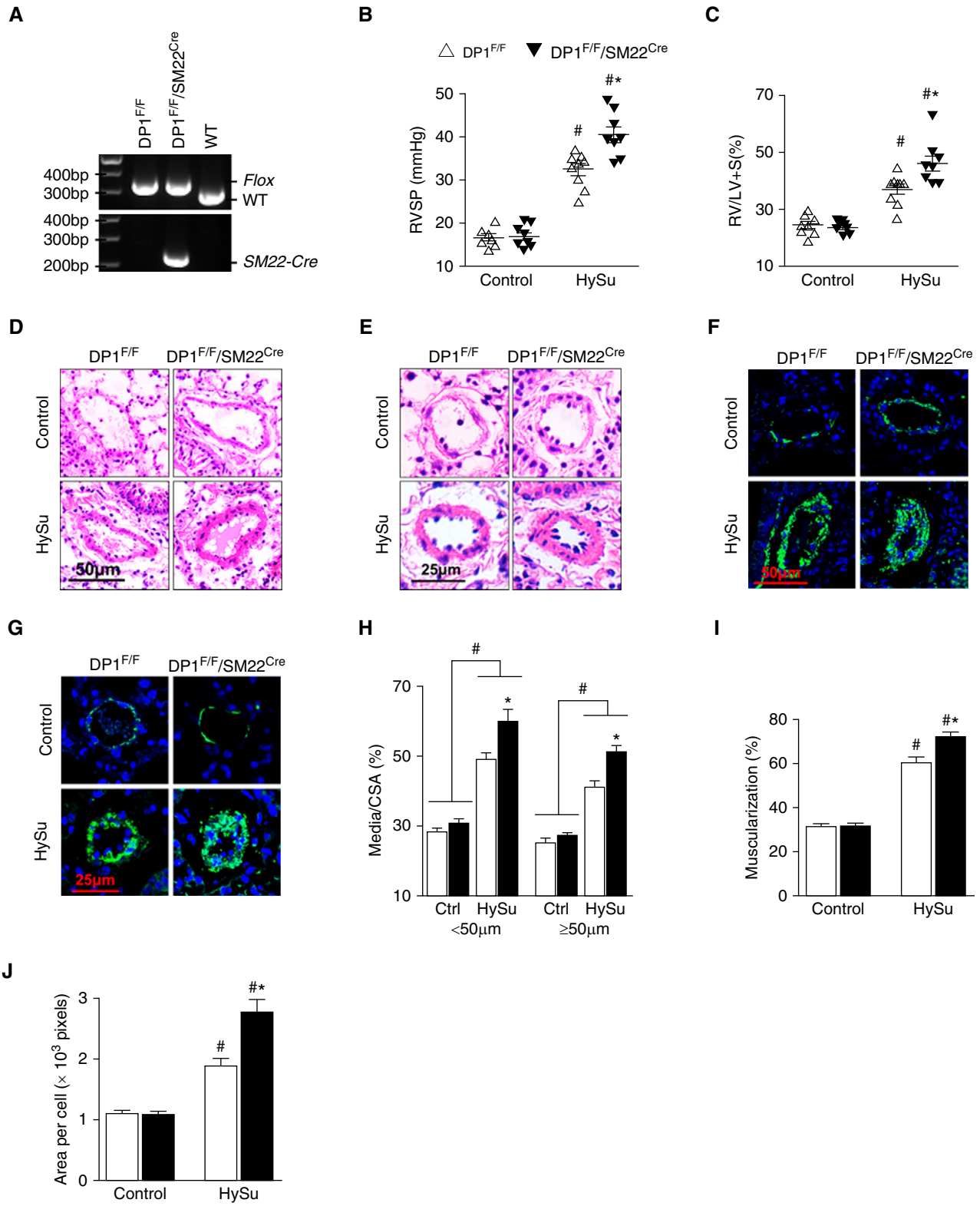

Figure 2. Vascular smooth muscle cell–specific DP1 (D prostanoid receptor subtype 1) deletion aggravates hypoxia-induced pulmonary arterial hypertension and pulmonary artery remodeling in mice. (*A*) Genotyping of vascular smooth muscle cell–specific DP1-knockout mice by PCR of genomic DNA extracted from tail biopsies. (*B*) Right ventricular systolic pressure (RVSP) in $DP1^{F/F}SM22^{Cre}$ and $DP1^{F/F}$ mice after hypoxia/SU5416 (HySu) treatment. $^{*}P < 0.05$ versus $DP1^{F/F}$ and $^{\#}P < 0.05$ versus control (Ctrl) ($n = 7$–9). (*C*) Weight of right ventricle/weight of left ventricle plus septum (RV/LV + S) in $DP1^{F/F}SM22^{Cre}$ and $DP1^{F/F}$ mice after HySu treatment. $^{*}P < 0.05$ versus $DP1^{F/F}$ and $^{\#}P < 0.05$ versus Ctrl ($n = 7$–9). (*D* and *E*)

its dissociation from raptor, although mTORC1 activity was restored by PKA inhibition (Figures 6B and 6C). Because raptor phosphorylation status determines mTORC1 activity (28, 29), we investigated whether raptor itself is a target of PKA. By aligning the raptor protein amino acid sequences of different species, we identified a conserved RRXS motif for PKA phosphorylation at Ser791 (Figure 6D). The *in vitro* kinase activity assay showed that the S791A raptor mutant was not phosphorylated by PKA (Figure 6E). Moreover, forskolin induced the phosphorylation of the PKA substrate motif in myc-tagged WT raptor but not the S791A mutant in transfected mPASMCs (Figure 6F). To further confirm PKA-mediated raptor phosphorylation, we developed an antibody that specifically recognizes the phosphorylated Ser791 site of raptor (Figure E16). DP1 agonist treatment enhanced raptor Ser791 phosphorylation and suppressed mTORC1 activity, whereas DP1 antagonist had the opposite effects (Figure 6G). The phosphorylation of raptor Ser791 in mPASMCs induced by DP1 agonist was associated with decreased binding to mTOR, but these effects were abolished by expression of S791A-mutant raptor (Figure 6H). Collectively, DP1 activation represses mTORC1 activity by promoting its complex dissociation through PKA-dependent Ser791 phosphorylation of raptor in PASMCs exposed to hypoxia (Figure 6I).

Treprostinil Ameliorates HySu-induced PAH in Mice by Activating Both IP and DP1

We then investigated whether treprostinil suppresses PAH development in part through activation of DP1. After 3 weeks of exposure to hypoxic conditions (10% O_2) and SU5416 administration, $IP^{-/-}$, $DP1^{-/-}$, and double-mutant ($IP^{-/-}DP1^{-/-}$) mice developed more severe PAH (Figures 7A and 7B) with aggravated PA remodeling, as evidenced by increased pulmonary vascular wall thickness and muscularization relative to control mice (Figures 7C–7F). Treprostinil treatment reversed the exacerbation of pulmonary hypertension and PA remodeling induced by HySu in $IP^{-/-}$ and $DP1^{-/-}$ mutants but not in $IP^{-/-}DP1^{-/-}$ mice (Figure 7). Indeed, treprostinil inhibited mTORC1 activity and downstream S6K phosphorylation in human PASMCs (Figure E17A) as well as in PAs from HySu-challenged mice (Figure E17B). Thus, treprostinil prevents the progression of PAH at least in part through activation of the DP1 receptor.

Discussion

The DP1 receptor mediates vasodilation of human arteries, including PAs (12, 30). In the present study, we found that DP1 was downregulated in PAs in rodent models of PAH and in patients with idiopathic PAH. *DP1* deficiency exacerbated hypoxia-induced PAH and enhanced PA remodeling in mice through activation of mTORC1 signaling. We determined that DP1 activation promoted mTORC1 dissociation and suppressed mTORC1 activity in PASMCs through PKA-mediated raptor phosphorylation. Thus, DP1 activation confers protection against hypoxia-induced PAH through PKA/raptor-dependent mTORC1 dissociation.

Increased contractility of small PAs and arterioles is a pathological feature of pulmonary hypertension. This is associated with heightened secretion of vasoconstrictor substances such as thromboxane and endothelin 1 and inhibition of vasodilator PGI_2 and nitric oxide release in patients with PAH (31–33). DP1 plays an important role in maintaining blood flow and hemostasis in rodents and humans, including brain blood flow after ischemia–reperfusion injury and nicotinic acid–induced vasodilation (30, 34). Despite the elevation in PGD_2 production in patients with primary PAH (35), we and others (11) have observed downregulation of DP1 in PAs in PAH rodent models. *DP1* deficiency intensified hypoxia-induced PAH and PA remodeling in mice, whereas DP1 agonist inhibited PAH progression in mice. In addition, infusion of large amounts of PGD_2 reversed pulmonary hypertension in newborn lambs (36). These results imply that decreased DP1 expression in PAs contributes to the pathogenesis of PAH.

mTOR is a member of the serine/threonine protein kinase family that regulates cell proliferation, protein synthesis, cell motility, gene transcription, and autophagy, and it also is the central component of mTORC1 and mTORC2. The two complexes are localized in different cellular organelles and have distinct functions (37): mTORC1 regulates protein synthesis and acts as a cellular nutrient, energy, and redox sensor, whereas mTORC2 regulates the actin cytoskeleton and cellular metabolism. PASMC proliferation and hypertrophy are major contributors to pulmonary vascular remodeling in PAH. The mTORC1 and mTORC2 pathways are both activated in PAs and isolated distal PASMCs from patients with idiopathic PAH, and they are required for PASMC proliferation induced by chronic hypoxia *in vivo* and *in vitro* (38). Pharmacological inhibition of mTOR kinases attenuates hypoxia-induced PA remodeling and right ventricular hypertrophy in rodents (39) and can improve PAH in patients (40). We found that *DP1* deficiency promoted PASMC proliferation and hypertrophy under hypoxic conditions and in pulmonary vessels of MCT-treated rats. However, we did not detect significant increases in PASMC proliferation in hypoxia-treated $DP1^{-/-}$ mice, likely due to the less severe pulmonary response induced by chronic hypoxia in mouse models (41). In agreement with the findings in $DP1^{-/-}$ mice, enhanced PASMC hypertrophy has also been reported in hypoxia-exposed

Figure 2. (*Continued*). Representative hematoxylin and eosin–stained sections of small pulmonary arteries and arterioles from HySu-treated $DP1^{F/F}SM22^{Cre}$ and $DP1^{F/F}$ mice. Scale bars, 50 and 25 μm in *D* and *E*, respectively. (*F* and *G*) Representative immunofluorescence images of α-SMA (α-smooth muscle actin) (green) expression in small pulmonary arteries (*F*) and arterioles (*G*) from HySu-treated $DP1^{F/F}SM22^{Cre}$ and $DP1^{F/F}$ mice. Scale bar, 50 μm. (*H*) Quantification of the ratio of vascular medial thickness to total vessel size for the HySu treatment model. $^{*}P < 0.05$ versus $DP1^{F/F}$ and $^{\#}P < 0.05$ versus Ctrl ($n = 8$ or 9). Scale bar, 25 μm. (*I*) Proportion of partially and fully muscularized pulmonary arteries (diameter = 20–50 μm) from HySu-treated mice. $^{*}P < 0.05$ versus $DP1^{F/F}$ and $^{\#}P < 0.05$ versus Ctrl ($n = 8$ or 9). (*J*) Quantification of pulmonary artery smooth muscle cell size in pulmonary arteries from HySu-treated $DP1^{F/F}SM22^{Cre}$ and $DP1^{F/F}$ mice. $^{*}P < 0.05$ versus $DP1^{F/F}$ and $^{\#}P < 0.05$ versus Ctrl ($n = 8$ or 9). Data represent mean ± SEM. Statistical significance was evaluated by two-way ANOVA with Bonferroni *post hoc* analysis. CSA = cross-sectional area; WT = wild type.

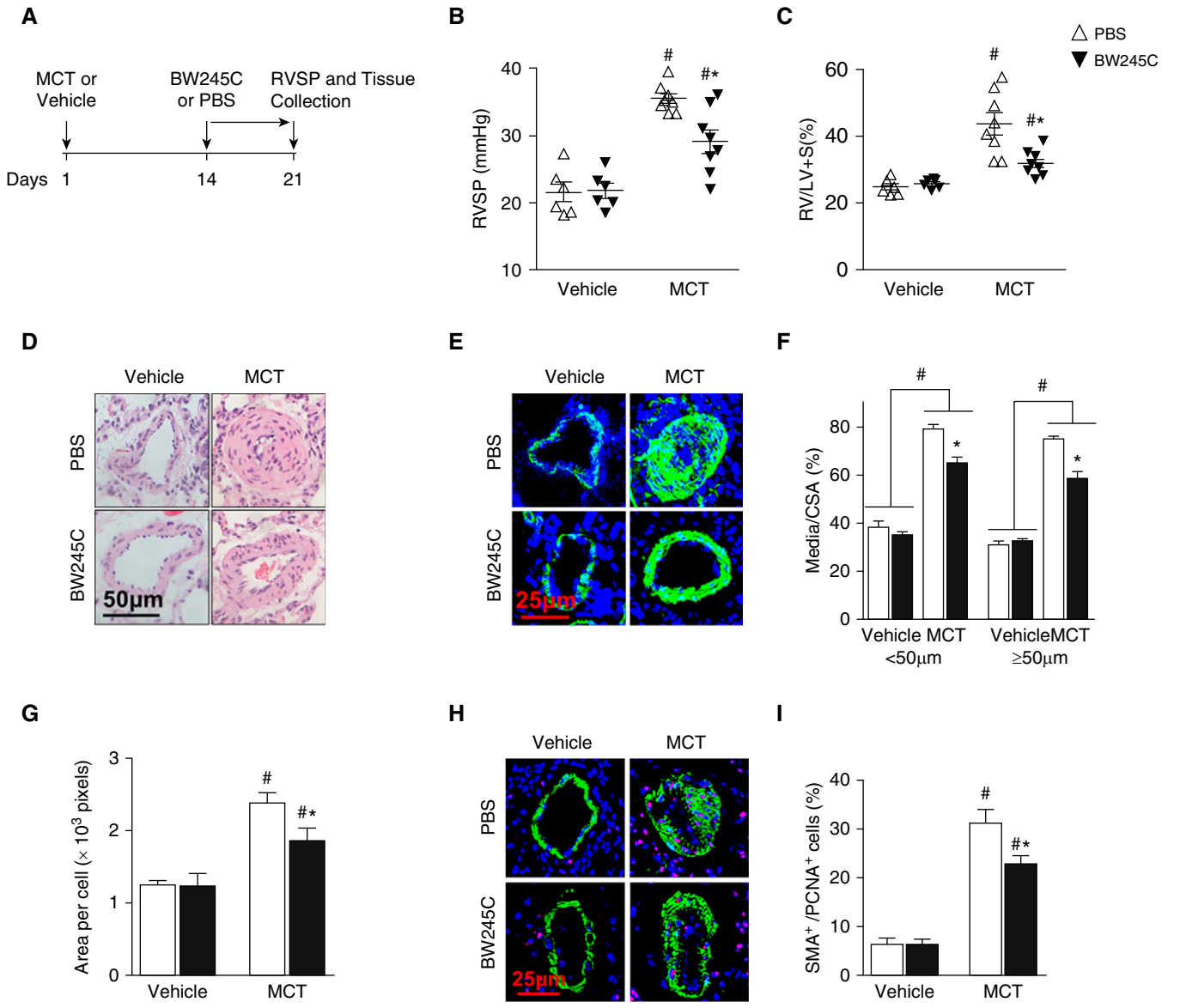

Figure 3. DP1 (D prostanoid receptor subtype 1) agonist treatment suppresses progression of monocrotaline (MCT)-induced pulmonary arterial hypertension in rats. (*A*) Protocol for administration of DP1 agonist BW245C to rats after MCT challenge. (*B* and *C*) Effect of BW245C administration on right ventricular systolic pressure (RVSP) and weight of right ventricle/weight of left ventricle plus septum (RV/LV + S) ratio in MCT-treated rats. $^{*}P < 0.05$ versus PBS and $^{\#}P < 0.05$ versus vehicle ($n = 6$–8). (*D*) Representative hematoxylin and eosin–stained lung sections of MCT-injected rats treated with BW245C. Scale bar, 50 μm. (*E*) Representative immunofluorescence images of α-SMA (α-smooth muscle actin) (green) expression in lung sections of MCT-injected rats treated with BW245C. Scale bar, 25 μm. (*F*) Quantification of the ratio of vascular medial thickness to total vessel size in MCT-challenged rats after BW245C treatment. $^{*}P < 0.05$ versus PBS and $^{\#}P < 0.05$ versus vehicle ($n = 6$–8). (*G*) Quantification of pulmonary artery smooth muscle cell size in the pulmonary arteries of MCT-challenged rats after BW245C treatment. $^{*}P < 0.05$ versus PBS and $^{\#}P < 0.05$ versus vehicle ($n = 6$–8). (*H*) Representative immunofluorescence images of α-SMA (green) and proliferating cell nuclear antigen (PCNA) (red) expression in lung sections of MCT-challenged rats after BW245C treatment. Scale bar, 25 μm. (*I*) Quantification of PCNA-positive cells in (*H*). $^{*}P < 0.05$ versus PBS and $^{\#}P < 0.05$ versus vehicle ($n = 6$–8). Data represent mean ± SEM. Statistical significance was evaluated by two-way ANOVA with Bonferroni *post hoc* analysis. CSA = cross-sectional area; PBS = phosphate-buffered saline.

COX-2–deficient mice (3). Interestingly, *DP1* deletion stimulated mTORC1 activity in hypoxia-treated mPASMCs without affecting activity of mTORC2, whereas rapamycin treatment abolished the enhancement of PAMSC hypertrophy and proliferation in *DP1*-deficient PASMCs, indicating that DP1 activation may alleviate hypoxia-induced PAH via suppression of mTORC1 signaling. However, DP1 expression and its downstream mTORC1 signaling alterations in treprostinil-treated patients with PAH warrant further investigation.

Raptor interacting with mTOR functions as a scaffold protein that facilitates the recruitment of substrates such as S6K1 and 4E-BP1 (eukaryotic

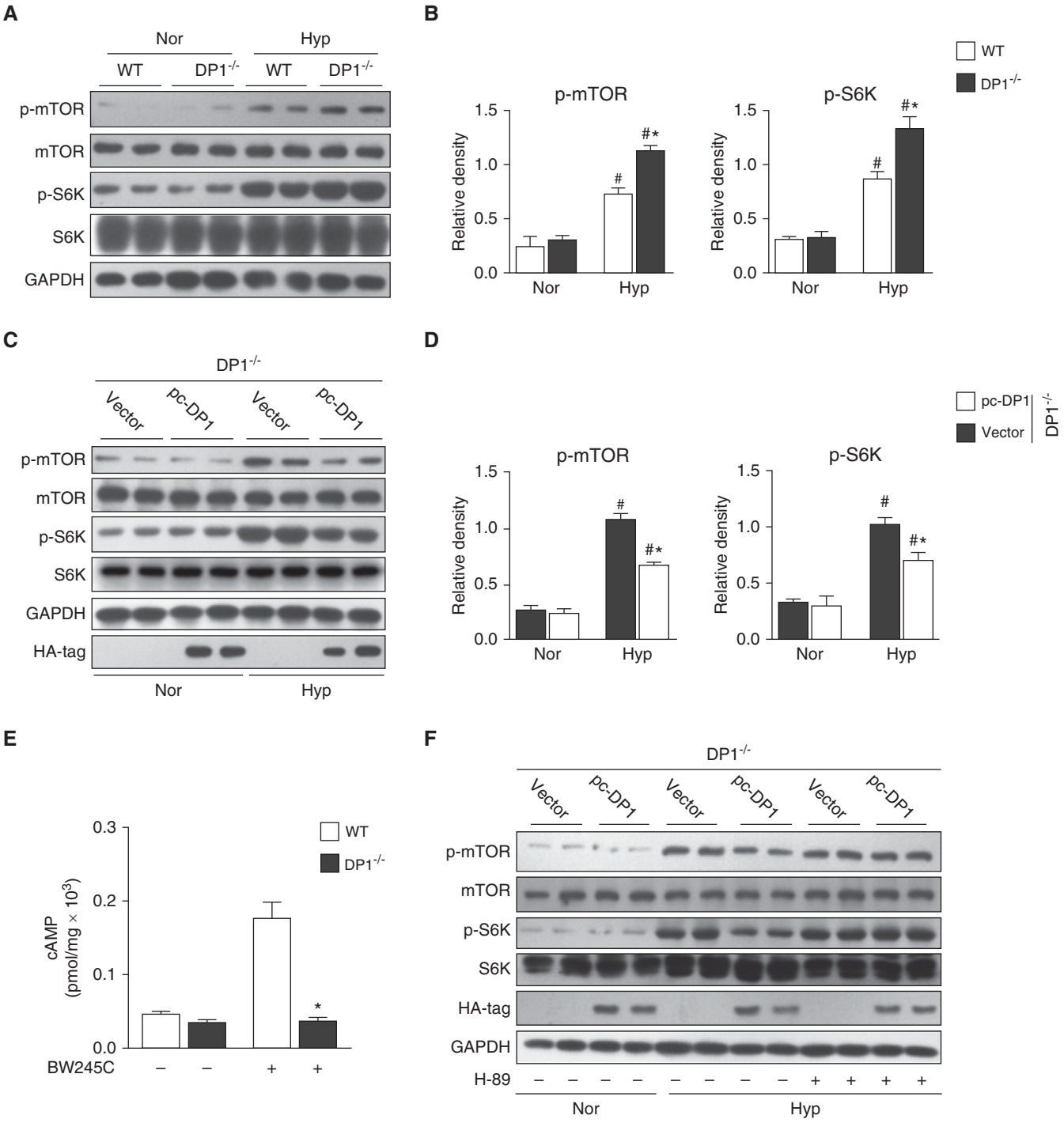

Figure 4. DP1 (D prostanoid receptor subtype 1) deficiency enhances mTOR (mammalian target of rapamycin) activity in pulmonary artery smooth muscle cells in response to hypoxia via cAMP/PKA (protein kinase A) signaling. (*A*) Expression levels of mTOR signaling components in cultured murine pulmonary artery smooth muscle cells (mPASMCs) under normoxia (Nor) or hypoxia (Hyp), as determined by Western blotting. (*B*) Quantification of p-mTOR (phosphorylated mTOR) and phosphorylated S6K (p-S6K) protein concentrations in *A*. $^{*}P < 0.05$ versus wild type (WT) and $^{\#}P < 0.05$ versus normoxia ($n = 4$). (*C*) Expression levels of mTOR signaling components in cultured DP1$^{-/-}$ mPASMCs with DP1 reexpression under normoxia or hypoxia, as determined by Western blotting. (*D*) Quantification of p-mTOR and p-S6K protein concentrations in *C*. $^{*}P < 0.05$ versus vector and $^{\#}P < 0.05$ versus normoxia ($n = 4$). (*E*) Effect of DP1 agonist BW245C treatment on intracellular cAMP concentrations in WT and DP1$^{-/-}$ mPASMCs. $^{*}P < 0.05$ versus WT ($n = 4$–6). (*F*) Effect of PKA inhibitor H-89 treatment (10 μmol/L) on mTOR signaling in cultured mPASMCs reexpressing DP1 under normoxia or hypoxia. Data represent mean ± SEM. Statistical significance was evaluated by two-way ANOVA with Bonferroni *post hoc* analysis. pc = pcDNA3.1 expression vector; HA-tag = hemagglutinin tag.

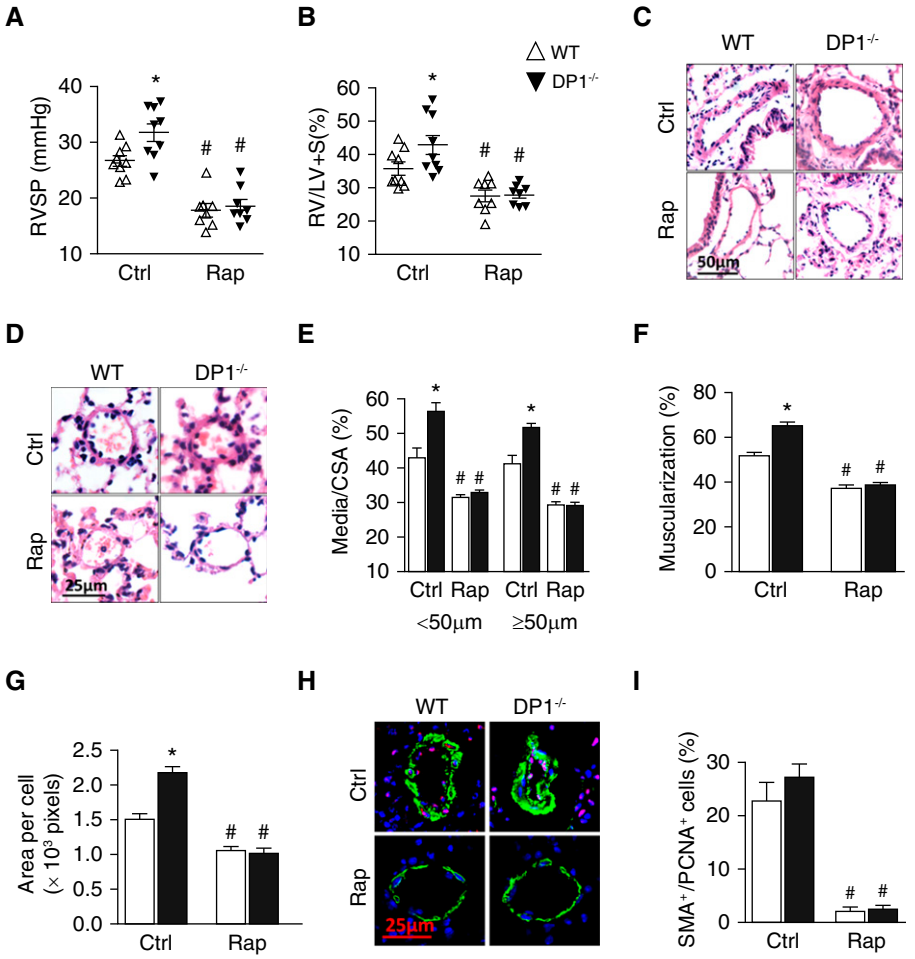

Figure 5. mTOR (mammalian target of rapamycin) inhibition attenuates pulmonary arterial hypertension exacerbation in hypoxia-exposed DP1$^{-/-}$ mice. (*A* and *B*) Effect of rapamycin (Rap) on right ventricular systolic pressure (RVSP) and weight of right ventricle/weight of left ventricle plus septum (RV/LV + S) ratio of hypoxia-treated mice. *$P < 0.05$ versus wild type (WT) and #$P < 0.05$ versus control (Ctrl) ($n = 8$ or 9). (*C* and *D*) Representative hematoxylin and eosin–stained sections of small pulmonary arteries and arterioles from hypoxia-challenged DP1$^{-/-}$ and WT mice after rapamycin treatment. (*E*) Quantification of the ratio of vascular medial thickness to total vessel size in hypoxia-challenged mice after rapamycin treatment. *$P < 0.05$ versus WT and #$P < 0.05$ versus Ctrl ($n = 7$–9). (*F*) Proportion of partially and fully muscularized pulmonary arterioles (20–50 μm in diameter) in hypoxia-exposed mice after rapamycin treatment. *$P < 0.05$ versus WT and #$P < 0.05$ versus Ctrl ($n = 8$ or 9). (*G*) Quantification of pulmonary artery smooth muscle cell size in pulmonary arteries from hypoxia-challenged mice after rapamycin treatment. *$P < 0.05$ versus WT and #$P < 0.05$ versus Ctrl ($n = 8$ or 9). (*H*) Representative immunofluorescence images of α-SMA (α-smooth muscle actin) (green) and proliferating cell nuclear antigen (PCNA) (red) expression in lung sections of hypoxia-challenged mice after rapamycin treatment. Scale bar, 25 μm. (*I*) Quantification of PCNA-positive cells in *H*. *$P < 0.05$ versus WT and #$P < 0.05$ versus Ctrl ($n = 6$ or 7). Data represent mean ± SEM. Statistical significance was evaluated by two-way ANOVA with Bonferroni *post hoc* analysis. CSA = cross-sectional area; DP1 = D prostanoid receptor subtype 1.

translation initiation factor 4E-binding protein 1) to mTORC1 (42). The integrity of mTOR complexes is critical for mTOR activity, and dissociation of raptor and mTOR protein suppresses the intrinsic catalytic activity of mTORC1 (26, 43). A three-dimensional structural analysis has shown that rapamycin inhibits mTORC1 by inducing the dissociation of raptor from mTOR complex (27). On the contrary, dissociation of the inhibitory component PRAS40 from the complex induced by AKT/PKB (protein kinase B)-mediated phosphorylation leads to induction of mTORC1 activity (44). We found that DP1 activation suppressed hypoxia-induced activation of mTORC1 by promoting raptor dissociation from mTOR in PASMCs. DP1 is coupled to $G_{\alpha s}$, and its activation leads to an increase in intracellular cAMP production. *DP1* deficiency caused a marked reduction in intracellular cAMP concentrations and, consequently, PKA activity in hypoxia-exposed PASMCs. Raptor phosphorylation is critical for mTORC1 activation, and multiple phosphorylation sites have been identified in raptor protein (28). For instance, raptor phosphorylation at Ser722/Ser792 is required for AMPK-mediated inhibition of mTORC1 activity (23). By mutagenesis experiments and using a phosphorylation-specific antibody, we and others (45) identified a conserved PKA phosphorylation site (Ser791) in raptor protein and showed that DP1 agonist treatment increased cellular cAMP generation and Ser791 phosphorylation in raptor, which promoted raptor dissociation from mTORC1. Mutation of Ser791 to Ala suppressed DP1 activation-induced dissociation of raptor from mTORC1 and reduced complex activity in PASMCs. In accordance with our findings, cAMP/PKA-dependent dissociation of mTORC1 and inhibition of mTORC1 have been observed in embryonic fibroblasts and HEK293 cells (25, 26), 3T3-L1 adipocytes (46), and lung fibroblasts (47). However, under some circumstances, PKA-driven mTORC1 activation is reported in mediation of the biological activities of hormones (e.g., catecholamine-stimulated adipose browning [45] and thyroid-stimulating hormone–induced proliferation [48]). In fact, the regulatory subunit of PKA (PRKAR1A [cAMP-dependent protein kinase type Iα regulatory subunit]) physically interacts with mTOR kinase and influences its autophosphorylation and activity (49), whereas the catalytic subunit of PKA directly phosphorylates mTOR kinase at different sites (45) and regulates mTOR substrates (50), thereby increasing the complexity of cross-talk between PKA and mTORC1. Thus, regulation of mTORC1 signaling by cAMP/PKA varies, depending on cell type and biological context.

In summary, DP1 activation slows the progression of PAH in rodents by PKA-mediated suppression of mTORC1 activity. Thus, targeting the DP1/PKA/mTORC1 pathway may represent a promising therapeutic strategy for the treatment of PAH. ■

Author disclosures are available with the text of this article at www.atsjournals.org.

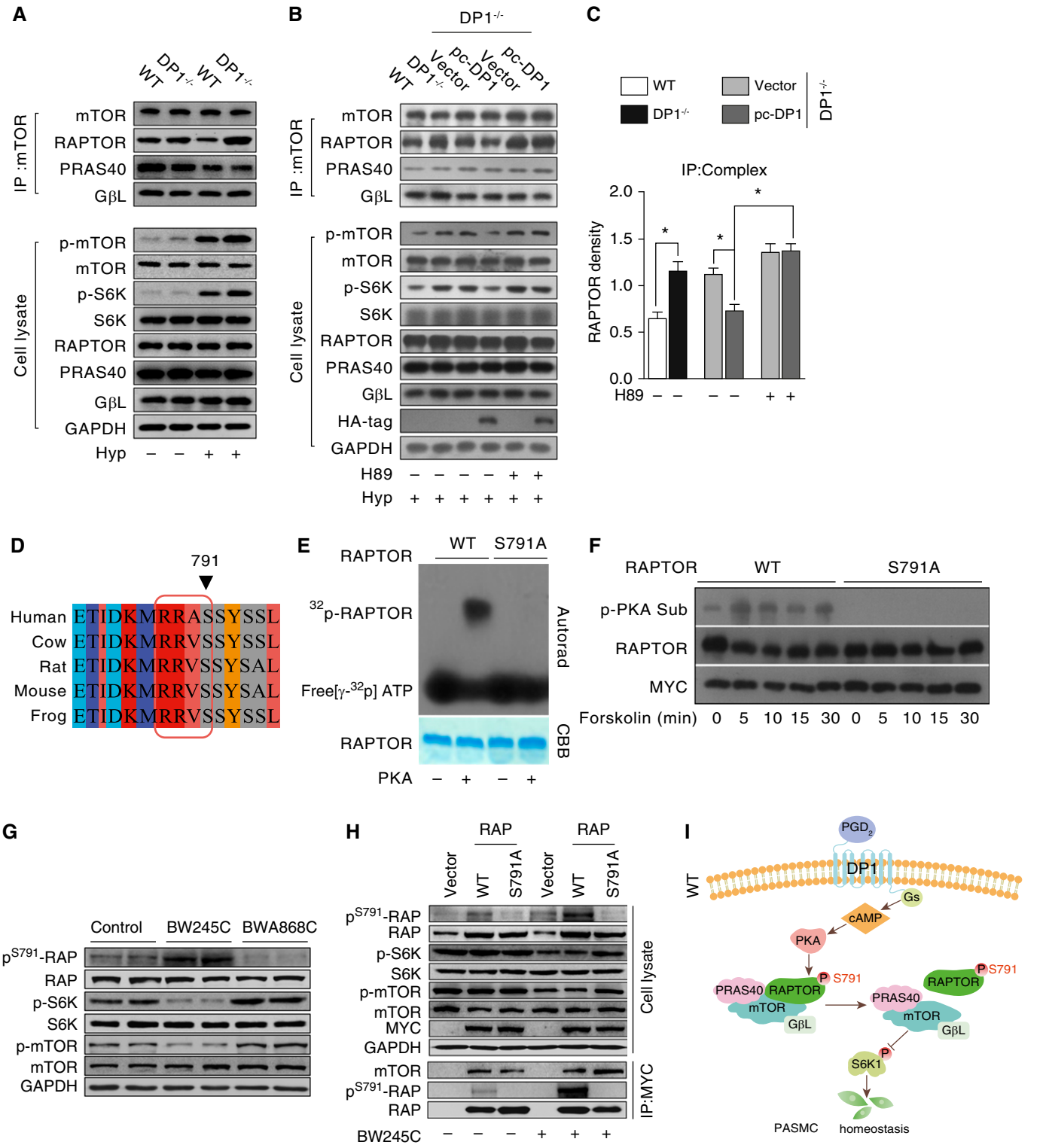

Figure 6. DP1 (D prostanoid receptor subtype 1) deficiency enhances mTORC1 (mammalian target of rapamycin complex 1) activity in hypoxia (Hyp)-treated murine pulmonary artery smooth muscle cells (mPASMCs) via PKA (protein kinase A)-induced raptor dissociation from mTORC1. (*A*) Expression levels of mTORC1 and signaling components in hypoxia-treated wild-type (WT) and DP1$^{-/-}$ mPASMCs, as determined by Western blotting. (*B*) Effect of PKA inhibitor H-89 (10 μmol/L) on the association of mTORC1 components in mPASMCs reexpressing DP1. (*C*) Quantification of mTOR–raptor association in *B*. *$P < 0.05$ versus indicated group ($n = 3$). (*D*) Amino acid sequence alignment of human, mouse, rat, cow, and frog raptor proteins. Ser791 is indicated by an arrowhead; box indicates phosphorylated PKA (p-PKA) substrate motif. (*E*) Top panel: Autoradiogram of ^{32}P-labeled recombinant WT raptor and Ser791→Ala (S791A) mutant protein after incubation with PKA. Bottom panel: Coomassie Blue–stained gel of raptor used for the above

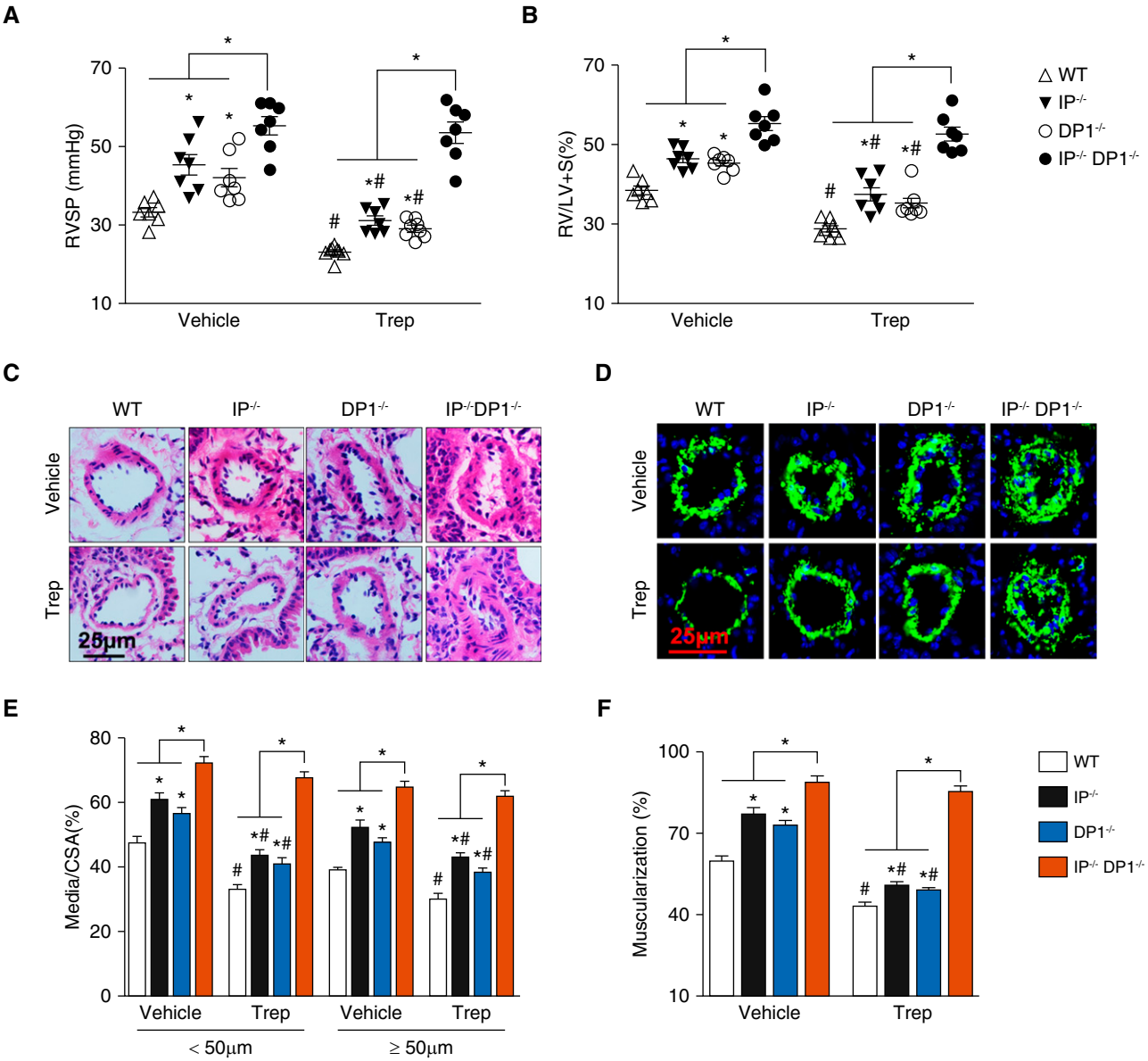

Figure 7. Treprostinil (Trep) protects against hypoxia/SU5416 (HySu)-induced pulmonary arterial hypertension in mice via activation of DP1 (D prostanoid receptor subtype 1) and prostaglandin I_2 (IP) receptors. (*A* and *B*) Right ventricular systolic pressure (RVSP) and weight of right ventricle/weight of left ventricle plus septum (RV/LV + S) ratio in HySu-challenged $DP1^{-/-}$, $IP^{-/-}$, $DP^{-/-}IP^{-/-}$, and wild-type (WT) mice with or without treprostinil treatment. $^{*}P < 0.05$ versus WT or as indicated and $^{\#}P < 0.05$ versus vehicle ($n = 7$ or 8). (*C* and *D*) Representative hematoxylin and eosin–stained lung tissue sections and immunofluorescence images of α-SMA (α-smooth muscle actin) (green) expression in lung tissue of HySu-challenged $IP^{-/-}$, $DP^{-/-}IP^{-/-}$, and WT mice with or without treprostinil treatment. Scale bar, 25 μm. (*E*) Quantification of the ratio of vascular medial thickness to total vessel size in HySu-challenged $DP1^{-/-}$, $IP^{-/-}$, $DP^{-/-}IP^{-/-}$, and WT mice with or without treprostinil treatment. $^{*}P < 0.05$ versus WT or as indicated and $^{\#}P < 0.05$ versus vehicle ($n = 7$ or 8). (*F*) Proportion of partially and fully muscularized pulmonary arterioles (diameter = 20–50 μm) in HySu-challenged $DP1^{-/-}$, $IP^{-/-}$, $DP^{-/-}IP^{-/-}$, and WT mice with or without treprostinil treatment. $^{*}P < 0.05$ versus WT or as indicated and $^{\#}P < 0.05$ versus vehicle ($n = 7$ or 8). Data represent mean ± SEM. Statistical significance was evaluated by two-way ANOVA with Bonferroni *post hoc* analysis. CSA = cross-sectional area.

Figure 6. (*Continued*). phosphorylation assay. (*F*) Western blot analysis of p-PKA substrate (RRXS*/T*) and raptor expression in forskolin-treated mPASMCs expressing myc-tagged WT and S791A mutant raptor. (*G*) Detection by Western blotting of phosphorylated raptor (p-raptor) (Ser791) and mTOR signaling components in mPASMCs after BW245C (0.5 μM) or BWA868C (10 μM) treatment. (*H*) Western blot analysis of p-raptor (Ser791)-induced raptor dissociation from mTORC1 in mPASMCs after BW245C treatment. (*I*) Schematic illustration of DP1-mediated PASMC homeostasis through PKA/raptor/mTORC1 signaling. Data represent mean ± SEM. Statistical significance was evaluated by two-way ANOVA with Bonferroni *post hoc* analysis. Autorad = autoradiogram; CBB = coomassie brilliant blue; HA-tag = hemagglutinin tag; IP = immunoprecipitation; pc = pcDNA3.1 expression vector; PGD_2 = prostaglandin D_2; Sub = substrates.

References

1. Rabinovitch M. Molecular pathogenesis of pulmonary arterial hypertension. *J Clin Invest* 2012;122:4306–4313.
2. Pullamsetti SS, Schermuly R, Ghofrani A, Weissmann N, Grimminger F, Seeger W. Novel and emerging therapies for pulmonary hypertension. *Am J Respir Crit Care Med* 2014;189:394–400.
3. Fredenburgh LE, Liang OD, Macias AA, Polte TR, Liu X, Riascos DF, *et al*. Absence of cyclooxygenase-2 exacerbates hypoxia-induced pulmonary hypertension and enhances contractility of vascular smooth muscle cells. *Circulation* 2008;117:2114–2122.
4. El Yafawi R, Wirth JA. What is the role of oral prostacyclin pathway medications in pulmonary arterial hypertension management? *Curr Hypertens Rep* 2017;19:97.
5. Kuwano K, Hashino A, Asaki T, Hamamoto T, Yamada T, Okubo K, *et al*. 2-[4-[(5,6-diphenylpyrazin-2-yl)(isopropyl)amino]butoxy]-*N*-(methylsulfonyl)acetamide (NS-304), an orally available and long-acting prostacyclin receptor agonist prodrug. *J Pharmacol Exp Ther* 2007;322:1181–1188.
6. Voswinckel R, Enke B, Reichenberger F, Kohstall M, Kreckel A, Krick S, *et al*. Favorable effects of inhaled treprostinil in severe pulmonary hypertension: results from randomized controlled pilot studies. *J Am Coll Cardiol* 2006;48:1672–1681.
7. Chen H, Rosenzweig EB, Gotzkowsky SK, Arneson C, Nelsen AC, Bourge RC. Treatment satisfaction is associated with improved quality of life in patients treated with inhaled treprostinil for pulmonary arterial hypertension. *Health Qual Life Outcomes* 2013;11:31.
8. Abramovitz M, Adam M, Boie Y, Carrière M, Denis D, Godbout C, *et al*. The utilization of recombinant prostanoid receptors to determine the affinities and selectivities of prostaglandins and related analogs. *Biochim Biophys Acta* 2000;1483:285–293.
9. Whittle BJ, Silverstein AM, Mottola DM, Clapp LH. Binding and activity of the prostacyclin receptor (IP) agonists, treprostinil and iloprost, at human prostanoid receptors: treprostinil is a potent DP_1 and EP_2 agonist. *Biochem Pharmacol* 2012;84:68–75.
10. Lu A, Zuo C, He Y, Chen G, Piao L, Zhang J, *et al*. EP3 receptor deficiency attenuates pulmonary hypertension through suppression of Rho/TGF-β1 signaling. *J Clin Invest* 2015;125:1228–1242.
11. Morrison K, Studer R, Ernst R, Haag F, Kauser K, Clozel M. Differential effects of selexipag and prostacyclin analogs in rat pulmonary artery. *J Pharmacol Exp Ther* 2012;343:547–555.
12. Walch L, Labat C, Gascard JP, de Montpreville V, Brink C, Norel X. Prostanoid receptors involved in the relaxation of human pulmonary vessels. *Br J Pharmacol* 1999;126:859–866.
13. Patel JA, Shen L, Hall SM, Benyahia C, Norel X, McAnulty RJ, *et al*. Prostanoid EP_2 receptors are up-regulated in human pulmonary arterial hypertension: a key anti-proliferative target for treprostinil in smooth muscle cells. *Int J Mol Sci* 2018;19:2372.
14. Benyahia C, Boukais K, Gomez I, Silverstein A, Clapp L, Fabre A, *et al*. A comparative study of PGI_2 mimetics used clinically on the vasorelaxation of human pulmonary arteries and veins, role of the DP-receptor. *Prostaglandins Other Lipid Mediat* 2013;107:48–55.
15. Kong D, Shen Y, Liu G, Zuo S, Ji Y, Lu A, *et al*. PKA regulatory IIα subunit is essential for PGD_2-mediated resolution of inflammation. *J Exp Med* 2016;213:2209–2226.
16. DuPage M, Dooley AL, Jacks T. Conditional mouse lung cancer models using adenoviral or lentiviral delivery of Cre recombinase. *Nat Protoc* 2009;4:1064–1072.
17. Paddenberg R, Stieger P, von Lilien AL, Faulhammer P, Goldenberg A, Tillmanns HH, *et al*. Rapamycin attenuates hypoxia-induced pulmonary vascular remodeling and right ventricular hypertrophy in mice. *Respir Res* 2007;8:15.
18. Kovacs L, Cao Y, Han W, Meadows L, Kovacs-Kasa A, Kondrikov D, *et al*. PFKFB3 in smooth muscle promotes vascular remodeling in pulmonary arterial hypertension. *Am J Respir Crit Care Med* 2019;200:617–627.
19. Nikam VS, Schermuly RT, Dumitrascu R, Weissmann N, Kwapiszewska G, Morrell N, *et al*. Treprostinil inhibits the recruitment of bone marrow-derived circulating fibrocytes in chronic hypoxic pulmonary hypertension. *Eur Respir J* 2010;36:1302–1314.
20. Loukanov T, Jaschinski C, Kirilov M, Klimpel H, Karck M, Gorenflo M. Cyclooxygenase-2 expression in lung in patients with congenital heart malformations and pulmonary arterial hypertension. *Thorac Cardiovasc Surg* 2013;61:307–311.
21. Stenmark KR, Fagan KA, Frid MG. Hypoxia-induced pulmonary vascular remodeling: cellular and molecular mechanisms. *Circ Res* 2006;99:675–691.
22. LoPiccolo J, Blumenthal GM, Bernstein WB, Dennis PA. Targeting the PI3K/Akt/mTOR pathway: effective combinations and clinical considerations. *Drug Resist Updat* 2008;11:32–50.
23. Gwinn DM, Shackelford DB, Egan DF, Mihaylova MM, Mery A, Vasquez DS, *et al*. AMPK phosphorylation of raptor mediates a metabolic checkpoint. *Mol Cell* 2008;30:214–226.
24. Hata AN, Breyer RM. Pharmacology and signaling of prostaglandin receptors: multiple roles in inflammation and immune modulation. *Pharmacol Ther* 2004;103:147–166.
25. Mavrakis M, Lippincott-Schwartz J, Stratakis CA, Bossis I. Depletion of type IA regulatory subunit (RIα) of protein kinase A (PKA) in mammalian cells and tissues activates mTOR and causes autophagic deficiency. *Hum Mol Genet* 2006;15:2962–2971.
26. Xie J, Ponuwei GA, Moore CE, Willars GB, Tee AR, Herbert TP. cAMP inhibits mammalian target of rapamycin complex-1 and -2 (mTORC1 and 2) by promoting complex dissociation and inhibiting mTOR kinase activity. *Cell Signal* 2011;23:1927–1935.
27. Yip CK, Murata K, Walz T, Sabatini DM, Kang SA. Structure of the human mTOR complex I and its implications for rapamycin inhibition. *Mol Cell* 2010;38:768–774.
28. Foster KG, Acosta-Jaquez HA, Romeo Y, Ekim B, Soliman GA, Carriere A, *et al*. Regulation of mTOR complex 1 (mTORC1) by raptor Ser863 and multisite phosphorylation. *J Biol Chem* 2010;285:80–94.
29. Wu XN, Wang XK, Wu SQ, Lu J, Zheng M, Wang YH, *et al*. Phosphorylation of Raptor by p38β participates in arsenite-induced mammalian target of rapamycin complex 1 (mTORC1) activation. *J Biol Chem* 2011;286:31501–31511.
30. Cheng K, Wu TJ, Wu KK, Sturino C, Metters K, Gottesdiener K, *et al*. Antagonism of the prostaglandin D_2 receptor 1 suppresses nicotinic acid-induced vasodilation in mice and humans. *Proc Natl Acad Sci USA* 2006;103:6682–6687.
31. Christman BW, McPherson CD, Newman JH, King GA, Bernard GR, Groves BM, *et al*. An imbalance between the excretion of thromboxane and prostacyclin metabolites in pulmonary hypertension. *N Engl J Med* 1992;327:70–75.
32. Giaid A, Saleh D. Reduced expression of endothelial nitric oxide synthase in the lungs of patients with pulmonary hypertension. *N Engl J Med* 1995;333:214–221.
33. Giaid A, Yanagisawa M, Langleben D, Michel RP, Levy R, Shennib H, *et al*. Expression of endothelin-1 in the lungs of patients with pulmonary hypertension. *N Engl J Med* 1993;328:1732–1739.
34. Ahmad AS. PGD_2 DP1 receptor stimulation following stroke ameliorates cerebral blood flow and outcomes. *Neuroscience* 2014;279:260–268.
35. Robbins IM, Barst RJ, Rubin LJ, Gaine SP, Price PV, Morrow JD, *et al*. Increased levels of prostaglandin D_2 suggest macrophage activation in patients with primary pulmonary hypertension. *Chest* 2001;120:1639–1644.
36. Soifer SJ, Morin FC III, Heymann MA. Prostaglandin D_2 reverses induced pulmonary hypertension in the newborn lamb. *J Pediatr* 1982;100:458–463.
37. Betz C, Hall MN. Where is mTOR and what is it doing there? *J Cell Biol* 2013;203:563–574.
38. Goncharov DA, Kudryashova TV, Ziai H, Ihida-Stansbury K, DeLisser H, Krymskaya VP, *et al*. Mammalian target of rapamycin complex 2 (mTORC2) coordinates pulmonary artery smooth muscle cell metabolism, proliferation, and survival in pulmonary arterial hypertension. *Circulation* 2014;129:864–874.
39. Pena A, Kobir A, Goncharov D, Goda A, Kudryashova TV, Ray A, *et al*. Pharmacological inhibition of mTOR kinase reverses right ventricle remodeling and improves right ventricle structure and function in rats. *Am J Respir Cell Mol Biol* 2017;57:615–625.
40. Wessler JD, Steingart RM, Schwartz GK, Harvey BG, Schaffer W. Dramatic improvement in pulmonary hypertension with rapamycin. *Chest* 2010;138:991–993.

41. Sztuka K, Jasińska-Stroschein M. Animal models of pulmonary arterial hypertension: a systematic review and meta-analysis of data from 6126 animals. *Pharmacol Res* 2017;125: 201–214.
42. Kim DH, Sarbassov DD, Ali SM, King JE, Latek RR, Erdjument-Bromage H, *et al*. mTOR interacts with raptor to form a nutrient-sensitive complex that signals to the cell growth machinery. *Cell* 2002;110:163–175.
43. Oshiro N, Yoshino K, Hidayat S, Tokunaga C, Hara K, Eguchi S, *et al*. Dissociation of raptor from mTOR is a mechanism of rapamycin-induced inhibition of mTOR function. *Genes Cells* 2004; 9:359–366.
44. Vander Haar E, Lee SI, Bandhakavi S, Griffin TJ, Kim DH. Insulin signaling to mTOR mediated by the Akt/PKB substrate PRAS40. *Nat Cell Biol* 2007;9:316–323.
45. Liu D, Bordicchia M, Zhang C, Fang H, Wei W, Li JL, *et al*. Activation of mTORC1 is essential for β-adrenergic stimulation of adipose browning. *J Clin Invest* 2016;126:1704–1716.
46. Scott PH, Lawrence JC Jr. Attenuation of mammalian target of rapamycin activity by increased cAMP in 3T3-L1 adipocytes. *J Biol Chem* 1998;273:34496–34501.
47. Okunishi K, DeGraaf AJ, Zasłona Z, Peters-Golden M. Inhibition of protein translation as a novel mechanism for prostaglandin E_2 regulation of cell functions. *FASEB J* 2014;28:56–66.
48. Blancquaert S, Wang L, Paternot S, Coulonval K, Dumont JE, Harris TE, *et al*. cAMP-dependent activation of mammalian target of rapamycin (mTOR) in thyroid cells: implication in mitogenesis and activation of CDK4. *Mol Endocrinol* 2010;24:1453–1468.
49. Mavrakis M, Lippincott-Schwartz J, Stratakis CA, Bossis I. mTOR kinase and the regulatory subunit of protein kinase A (PRKAR1A) spatially and functionally interact during autophagosome maturation. *Autophagy* 2007;3:151–153.
50. Lécureuil C, Tesseraud S, Kara E, Martinat N, Sow A, Fontaine I, *et al*. Follicle-stimulating hormone activates p70 ribosomal protein S6 kinase by protein kinase A-mediated dephosphorylation of Thr 421/Ser 424 in primary Sertoli cells. *Mol Endocrinol* 2005;19:1812–1820.